AMYLOIDOGENIC INTRINSICALLY DISORDERED PROTEINS: CONFORMATIONAL PLASTICITY, MEMBRANE BINDING AND AGGREGATION

KARISHMA BHASNE

A dissertation submitted for the partial fulfillment of

BS-MS dual degree in Science

Department of Biological Sciences

Indian Institute of Science Education and Research (IISER) Mohali

April 2013

Certificate of Examination

This is to certify that the dissertation titled "Amyloidogenic intrinsically disordered proteins: Conformational plasticity, membrane binding and aggregation" submitted by Ms. Karishma Bhasne (MS08028) for the partial fulfilment of BS-MS dual degree programme of the Institute, has been examined by the thesis committee duly appointed by the Institute. The committee finds the work done by the candidate satisfactory and recommends that the report be accepted.

Prof. Purnananda Guptasarma Dr. Rachna Chaba Dr. Samrat Mukhopadhyay

(Supervisor)

Declaration

The work presented in this dissertation has been carried out by me under the supervision of Dr. Samrat Mukhopadhyay at the Department of Biological Sciences, Indian Institute of Science Education and Research (IISER) Mohali.

This work has not been submitted in part or full for a degree, a diploma, or a fellowship to any other university or institute.

Whenever contributions of others are involved, every effort is made to indicate this clearly, with due acknowledgement of collaborative research and discussions. This thesis is a bona fide record of original work done by me and all sources listed within have been detailed in the bibliography.

Date Karishma Bhasne

In my capacity as supervisor of the candidate's thesis work, I certify that the above statements by the candidate are true to the best of my knowledge.

Dr. Samrat Mukhopadhyay

(Supervisor)

Acknowledgements

This is the best section of any thesis, because one can express gratitude without restrictions. I truly want to acknowledge Dr. Samrat Mukhopadhyay for his valuable guidance in my professional and personal development. The first thing which I enjoyed in the lab is the "intellectual freedom" that he gives to his students that made everyone capable of designing the experiments. He is full of energy and is capable of EET (Enthusiasm and Energy Transfer) with almost 100% efficiency. He often says "Sky is the limit" which is the most inspiring sentence for a student. His enthusiasm, guidance, support, patience, innovative ideas and experience has changed my scientific outlook. His knowledge is not only confined to his area of research but also in other areas of science, which makes his talks more enjoyable. Sometimes it is frustrating when experiments do not work but his phrase "Experiments do not work, we have to make them work" always inspired me to think in a different way to approach the problems.

I would like to thank Dr. Mily Bhattacharya for being a role model of a woman in science and an extraordinary inspiring personality. She is the first person who introduced me the basics of research and has taken me to the advanced level. According to her "There is always some logic in doing science" which always motivated me to think logical. She always inspires me to think out of the box. I will always be thankful to her for her help not only in professional pursuits but also in personal life. She is one among the best teachers I have ever been taught in my life.

My project would have been almost impossible without the urging of Neha Jain. Her advice and personal attention shepherded me throughout my tenure. She had initiated the work on α-synuclein and has taught me everything related to this protein. Almost all the work which I did was always supported by her. She has helped me greatly in designing the biophysical experiments of Tau and α-synuclein co-aggregation. Her immense love and care always made me smile during the toughest phase. I

would also like to thank her for recording tryptophan fluorescence anisotropy decays carried out at TIFR Mumbai and also for her help with the data analysis. I thank Prof. G. Krishnamoorthy (TIFR) for allowing Neha to record the data and Prof. N. Periasamy (TIFR) for providing us with the decay analysis software.

I am also grateful to Dominic Narang for teaching me the basics of molecular biology. My scientific development would have been impossible without Vijit, Shruti, Arpana, Hema, Anubhuti, Priyanka, Ritu, Shwetha and other past members of The Mukhapadhyay Lab. Their suggestions and discussions have helped me in shaping my thesis in a better form.

I am also thankful to Prof. Vinod Subramaniam (University of Twente, The Netherlands) for kindly providing us with the α-synuclein plasmid and Prof. Elizabeth Rhodes for providing us with the Tau (k18) plasmid. I am grateful to the Department of Science and Technology, Govt. of India, for the DST-INSPIRE fellowship. I am thankful to IISER Mohali for providing all the facilities for my research.

Life would not have been so cheerful without the friends. I enjoyed my most of the time with Neha, Amol, Neeraj, Nitish, Anuj, Aditya, Chandrakala, Akansha, Priyanka, Shashank, Shikha, Rajveer, Neelam, Anshu, Mehreen and Abhilasha.

Last, but not the least I thank the most important people of my life, my parents and my brother Himanshu for their constant love and encouragement. I would like to especially thank my cousin, Sachin, who always helped me in every step of my life and made my life as beautiful as one can think of. He taught me each and every small thing which is important for the overall development. I would like to thanks him for his immense love and care. In addition to that I am grateful to my Aunty, uncle and my cousin Parv and Nipurn for their love……

List of Figures

Figure 10. Schematic representation (a) Unbound α-synuclein (b) α-synuclein bound to membrane.

Figure 11. (a) Sequence of Tau (k18) (b) A schematic map of full length Tau (c) Tau (k18) protein pure fractions.

Figure 12. (a) Control experiment (with only Tau and only α-synuclein). (b) Tau : α-synuclein ratio 2:1 (c) Tau : α-synuclein ratio 4:1 and (b) Tau : α-synuclein ratio 5:1

List of table

Contents

Amyloidogenic intrinsically disordered proteins: Conformational plasticity, membrane binding and aggregation

Karishma Bhasne

Department of Biological Sciences

Indian Institute of Science Education and Research (IISER), Mohali

M.S. Thesis Supervisor: Dr. Samrat Mukhopadhyay

Abstract:

Natively unfolded or intrinsically disordered proteins (IDPs) possess astonishing conformational plasticity that allows them to adopt a wide range of structures. My work involves the study of two amyloidogenic IDPs, namely α-synuclein and tau, aggregation of which are involved in Parkinson's and Alzheimer's diseases, respectively. α-synuclein adopts a helical structure upon binding to the membranes. However, the high-resolution structural and dynamical insights of the membrane bound α-synuclein remain elusive. We took the advantage of the fact that α-synuclein does not have any tryptophan and incorporated single Trp mutant along the polypeptide chain. These Trp mutants of the α-synuclein have been used as a crucial scout. The fluorescence anisotropy map illuminates the structural rigidification of various regions of the polypeptide chain mediated by membrane binding-induced folding. In order to obtain the depth-profile of different segments of α-synuclein from the membrane surface, we utilized a unique and reliable indicator, such as red-edge excitation shift (REES), which is utilized to monitor the dynamics of restricted water molecules at the membrane-water interface.[1,2] The membrane-water interface comprises of ~ 15 Å thick water layers having strongly bound (restrained) water (also known as biological water) and has been hypothesized to play a pivotal role in a variety of crucial biomolecular processes. In order to achieve the distance profile between the membrane surface and the protein residues, we have used fluorescence resonance energy transfer (FRET) experiments between fluorescently labeled membrane and Trp locations of α-synuclein. Taking together all the results from these fluorescence readouts, we have proposed a model that elucidates the precise conformation of the α-synuclein protein on the negatively charged membrane. Additionally, we have also investigated the influence of α-synuclein in the amyloid aggregation of tau protein that is implicated in human neurodegenerative disorders.

1. Introduction:

Intrinsically Disorder Proteins (IDPs) do not follow the conventional sequence-structure-function paradigm.[3] IDPs being conformational plastic can adopt different structures depending upon their binding partners such as ligands and membranes. This property of IDPs makes them more useful in a wide range of physiological functions involving cell-signaling, transcription, etc.[4] α-synuclein is mainly found in presynaptic terminals of neurons in the brain and the central nervous system (CNS). It is a small protein of 140 amino acids and the complete sequence is divided into three distinct regions (Figure 1) : N-terminal (1-60 amino acid) which has an affinity to bind to the membranes, central region (61-95 amino acid) known as NAC region (non-amyloid β component of Alzheimer disease amyloid) which initiates the aggregation[5] and the third region C-terminal (96-140 amino acid) is highly negatively charged and it facilitates the binding of calcium and other ions).[6] The exact function of α-synuclein protein is poorly understood, though, there are few proposed functions known such as synaptic transmission[7], synaptic vesicle localization[8], maintenance of neuronal plasticity[9] etc. The synaptic transmission mechanism by SNARE complex is not clearly understood. SNARE complex is the group of proteins that helps in the vesicle fusion to the presynaptic terminal, which results in the neurotransmitter release to the presynaptic cleft. It has been evident that α-synuclein interacts with the SNARE complex protein of the presynaptic terminal of the axon. Many biophysical experiments have been performed to understand the interaction between membrane (mimic as presynaptic terminal) and α-synuclein, the results showed that α-synuclein undergoes a conformational change from random coil to alpha helical structure.[10] Numerous studies have led to the conclusion that α-synuclein can exist either in broken helix (horseshoe)[11,12] or extended helix form.[12] But the in-depth residue-specific information of the membrane bound α-synuclein is still remains exclusive. Therefore, in order to understand the residue specific structural details, we have employed a variety of fluorescence techniques such as fluorescence anisotropy, red-edge excitation shift (REES), time-resolved emission spectra (TRES) and fluorescence resonance energy transfer (FRET). We took the advantage that α-synuclein does not have any tryptophan and incorporated single Trp residue along the polypeptide chain using site-directed mutagenesis. These Trp mutants of the α-synuclein have been used as a crucial scout. The fluorescence anisotropy map illuminates the structural rigidification of various regions of

the polypeptide chain mediated by membrane binding-induced folding. In order to obtain the structural underpinnings and the depth-profile of different segments of α-synuclein from the membrane surface, we utilized a unique and reliable indicator, such as REES, which is utilized to monitor the dynamics of restricted water molecules at the membrane interface.[1,2] The membrane-water interface comprises of ~ 15 Å thick water layers having strongly bound (restrained) water (also known as biological water) and has been hypothesized to play a pivotal role in a variety of crucial biomolecular processes. In order to achieve the distance profile between membrane and protein we have used FRET experiments between NBD-PE (1,2-dipalmitoyl-sn-glycero-3-phosphoethanolamine-N-(7-nitro-2-1,3-benzoxadiazol-4-yl)) labeled membrane and Trp of α-synuclein. Taking together all the results from these fluorescence readouts, we have proposed a model, which elucidates the precise conformation of the α-synuclein protein on the negatively charged membrane.

Tau is also an amyloidogenic IDP that is found mostly in the CNS. It is a highly soluble microtubule binding protein, which interacts with tubulin protein and stabilizes the polymerization of tubulin protein. In human brain tissues, six different isoforms of Tau are present which are different in the number of microtubule binding domains (repeats).[13] Hyperposphorylation of Tau protein at specific position results in the self assembly which leads to the formation of tangles of paired helical filaments (PHF)[14] that are involved in Alzheimer's disease. It has been shown that Tau and α-synuclein are colocalized in many diseases like multiple system atrophy, Pick's disease, Parkinson's disease, etc.[15] The colocalization of these two proteins also result in the formation of aggregates which results in the neuronal degradation and finally results in dementia.[16] We aim to answer some fundamental questions pertaining to the co-aggregation of Tau and α-synuclein which will help to understand the molecular mechanism in great detail.

2. Experimental Section:

2.1 Materials:

Chloroform solutions of POPG (1-palmitoyl-2-oleoyl-snglycero-3-phospho (1'-rac-glycerol)) and NBD-PE (1,2-dipalmitoyl-sn-glycero-3-phosphoethanolamine-N-(7-nitro-2-1,3-benzoxadiazol-4-yl) (ammonium salt)) were purchased from Avanti Polar Lipids. di-8-ANEPPS (di-8-butyl-amino-naphthyl-ethylene-pyridinium-propyl-sulfonate) was purchased from Invitrogen. LB (luria broth mixture powder), agar powder, tris, glycine, SDS (sodium dodecyl sulphate), NaCl (sodium chloride), lysozyme and $MgCl_2$ (magnesium chloride) were purchased from Hi-Media. EDTA (ethylenediaminetetraacetic acid), protease inhibitor cocktail, HEPES (4-(2-hydroxyethyl) piperazine-1-ethanesulfonic acid), KI (potassium iodide), MES (2-(N-morpholino) ethanesulfonic acid), DTT (dithiothreitol), SP (sulfopropyl) sepharose fast flow resin, $MgSO_4$ (magnesium sulphate), glucose and ThT (thioflavin T) were purchased from Sigma and used as received. Ampicillins, chloramphenicol and IPTG (isopropyl β-D-1-thiogalactopyranoside) were purchased from Goldbio.Com. HCl (hydrochloric acid), $CaCl_2$ (calcium chloride), ethanol, glacial acetic acid and ammonium sulphate were purchased from Merck. Q (quaternary ammonium) sepharose fast flow resin was purchased from GE Healthcare and streptomycin sulphate was purchased from CDH and used as received.

2.2 Protein Expression and Purification:

2.2.1 α-synuclein:

Wild-type and mutant α-synuclein were purified using a reported protocol.[17] The pT7-7 plasmid with α-synuclein gene was kindly provided by Prof. Vinod Subramaniam from the University of Twente, The Netherlands. It was transformed in BL21 (DE3) strain of *Escherichia coli*. Briefly, 1 % of the overnight grown culture (containing 100 μg/mL ampicillin and 35 μg/mL chloramphenicol) of BL21 (DE3) was transferred into fresh media (containing 100 μg/mL ampicillin) and when the O.D at 600 nm reached to 0.6 - 0.8, the cells were induced with 800 μM IPTG for 4 hours. To obtain the cell pellet, culture was centrifuged at 4,000 rpm for 30 min at 4 °C. Pellet was resuspended in lysis buffer (50 mM Tris, 150 mM NaCl, 10 mM EDTA, pH 8 containing 50 μL protease

inhibitor cocktail). And stored at -80 °C till further use. The lysed cells were boiled at 95 °C for 30 min followed by centrifugation at 12,000 rpm for 30 min at 4 °C. The supernatant was collected and thoroughly mixed with 136 µL/mL of 10 % streptomycin sulphate and 228 µL/mL of glacial acetic acid followed by centrifugation at 12,000 rpm for 30 min at 4 °C. To the clear supernatant, equal volume of saturated ammonium sulphate was added and kept at 4 °C with an intermittent mixing for 1 hour. The precipitated protein, separated by centrifugation at 12,000 rpm for 30 min at 4 °C was suspended in equal volume of 100 mM ammonium acetate and ethanol followed by centrifugation at 4,000 rpm for 10 min at 4 °C. Finally, the pellet was washed twice with absolute ethanol and dried at room temperature, until ethanol evaporated. The pellet was suspended in equilibrating buffer (10 mM Tris, pH 7.4) and further purified by FPLC (fast performance liquid chromatography) on a Q Sepharose column and the protein was eluted at ~ 300 mM NaCl. The purity of the collected fractions was assessed by SDS-PAGE (SDS - polyacrylamide gel electrophoresis) (Figure 1). The pure fractions were dialyzed in a dialysis buffer (10 mM HEPES, 50 mM NaCl, pH 7.4) and stored at -80°C.

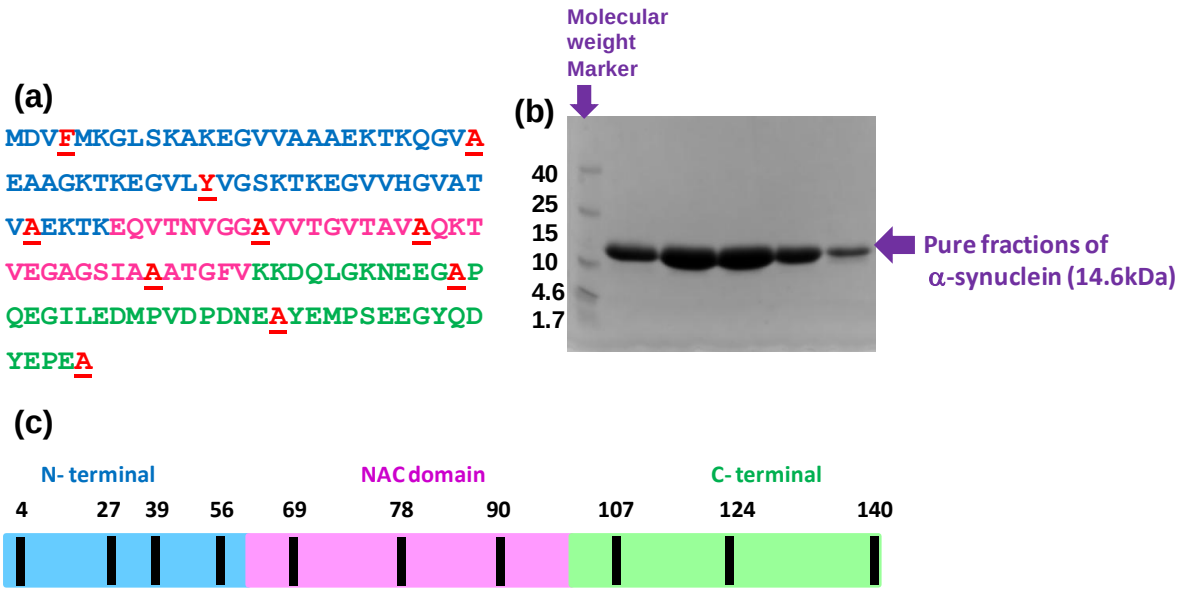

Figure 1. (a) Sequence of α-synuclein showing distribution of charged amino acids. Residues underlined were replaced by tryptophan (b) SDS-PAGE showing fractions of pure α-synuclein (c) Different regions of α-synuclein with mutant positions highlighted in black.

2.2.2 Tau k18 fragment:

The plasmid pET11a containing Tau (k18) gene was kindly provided by Prof. Elizabeth Rhodes from the Yale University, New Haven, USA. Tau k18 fragment was expressed and purified in the similar manner as α-synuclein, except that the buffer and column used were different. Lysis buffer composition: protease inhibitor cocktail, lysozyme (12 mg / 60 mL), 500 mM NaCl, 50 mM Tris buffer pH 8 and Equilibrating buffer: 20 mM MES, 1 mM EDTA, 2 mM DTT and 1 mM $MgCl_2$. The SP sepharose (strong cation) column was used and the protein was purified by FPLC and eluted at ~ 300 mM NaCl. The pure fractions were assayed on SDS-PAGE (Figure 11) and dialyzed in a dialysis buffer (MES 20 mM, $MgCl_2$ 1 mM, DTT 2 mM and EDTA 1 mM, pH 6.8) and stored at -20°C.

2.3 Preparation of protein samples: (α-synuclein)

Prior to every experiment the wild type and single Trp mutants of α-synuclein were passed through 50 kDa molecular weight cut-off (MWCO) AMICON filter (purchased from Millipore) and concentrated using 3 kDa MWCO AMICON. The concentration of proteins was by measuring tryptophan absorbance using UV-Vis spectrophotometer (Chirascan, Applied photophysics)). The concentration of wild-type protein was determined using ε_{275}=5,600 $M^{-1}cm^{-1}$.[17] Concentration for all the mutants (except Y39W) was determined using ε_{280} =10,810 $M^{-1}cm^{-1}$, whereas, for Y39W ε_{280} = 9,970 $M^{-1}cm^{-1}$. [18] The measurements were carried out using 1 mm pathlength cuvette with a scan range of 260-300 nm and a scan rate of 1 nm/s. The final spectra were averaged over 2 scans and buffer subtracted. The purified proteins were stored at -80 °C.

2.4 Preparation of small unilamellar vesicles (SUV)

Small unilamellar vesicles (SUVs) (diameter ~ 35 nm) from anionic POPG were prepared using a reported protocol.[19] Briefly, appropriate amount of the respective chloroform solution was taken in a round bottom flask and purged with a gentle stream of nitrogen for 1 hour followed by vacuum desiccation for 2 hours to ensure complete removal of the residual organic solvent. The dried lipid film was hydrated in DPBS (Dulbecco's phosphate buffer saline: 2.67 mM KCl, 1.47 mM KH_2PO_4, 138 mM NaCl, and 8.06 mM Na_2HPO_4, pH 7.4) buffer with intermittent vortexing for 1 hour to a final lipid

concentration of 10 mM. This resulted in a turbid solution having MLVs (multilamellar vesicles). The MLVs were subjected to 5 freeze-thaw cycles, alternating between liquid nitrogen and water bath (preset at 42 °C) for one minute. The MLVs were then sonicated in a bath sonicator for 1 hour at 40 °C using 37 Hz pulse rate to obtain SUVs. The size of the SUVs (35 nm ± 10 nm) was confirmed by DAWN 8 Helios MALS system (Wyatt Technology). The fluorescently labeled SUVs were prepared in the similar manner as the unlabeled SUVs. 5 % of NBD-PE (chloroform solution) was added into the chloroform solution stock of POPG before proceeding for lipid film formation. The labeled liposomes were kept protected from light.

2.5 Tau and α-synuclein co-aggregation:

Tau and α-synuclein co-aggregation was carried out using different ratiometric concentrations of Tau and α-synuclein (1:2, 1:4 and 1:5). The aggregation reaction was setup in 14 mM MES buffer (pH 6.8) with 200 rpm agitation, on a stirrer that was preset at 37 °C. Aliquots of the aggregation reaction were taken out at regular intervals, diluted to a 5 μM concentration of Tau using a buffer (14 mM, MES, pH 6.8), and allowed to cool at room temperature prior to ThT fluorescence measurements. ThT was used as an indicator for aggregation. For aggregation experiments, ThT concentration of 20 μM was used which was obtained by suitable dilution of a stock solution (1 mM) of ThT (prepared in Milli-Q water and stored at 4 °C) into the aliquot of aggregation solution and the spectra were collected using the following parameters: λex = 450 nm, λem (range) = 460-520 nm, excitation bandpass = 1.5 nm, emission bandpass = 4.5 nm and scan rate was fixed at 1 nm/s.

2.6 Circular Dichroism (CD) experiments:

The CD spectra were collected on Chirascan CD spectrometer (Applied Photophysics, UK) using a 1 mm path length quartz cuvette at room temperature. The concentration of wild-type and mutants of α-synuclein were fixed as 25 μM. CD spectra in the absence and in the presence of POPG (1 mM) in DPBS buffer were collected with a scan rate of 1 nm/s and averaged over 3 scans. The scan range was fixed from 200 nm to 260 nm. All the spectra were buffer subtracted and smoothened using Chirascan 'ProData viewer' software provided with the instrument.

2.7 Steady state-fluorescence measurements:

All steady state experiments were carried out on Fluoromax-4 (Horiba Jobin Yvon, NJ) using 10 mm x 2 mm quartz cuvette at room temperature. For anisotropy experiments, the concentration of all mutants of α-synuclein and SUVs were fixed at 50 μM and 2 mM respectively. The steady-state anisotropy is given by:

$$r = (I_{||} - GI_{\perp}) / (I_{||} - 2GI_{\perp}), \quad (1)$$

where $I_{||}$ and $I_{\perp}$ are fluorescence intensities collected using parallel and perpendicular geometry of the polarizers, respectively and the perpendicular components were corrected using respective G-factors. For anisotropy measurements, excitation wavelength and bandpass were fixed to 295 nm and 1 nm, respectively, whereas emission wavelength was fixed at the maxima for each mutant with a bandpass of 5 nm. The integration time was fixed as 3 s.

2.7.1 REES (Red Edge Excitation Shift) POPG experiments:

For REES experiments, the concentration of α-synuclein Trp variants and SUVs were taken as 50 μM and 2 mM, respectively. Following parameters were adjusted for collecting tryptophan emission spectra; λ_{ex} = 280/295/305 nm and λ_{em} (scan range) = 310 nm to 400 nm. The excitation bandpass was adjusted to 0.5 nm (for λ_{ex} = 280 nm and 295 nm) and 1 nm (for λ_{ex} = 305 nm). The emission bandpass was fixed to 3 nm. For λ_{ex} = 280 nm and 295 nm, the integration time was fixed to 1 s and averaged over three scans, whereas, for λ_{ex} = 305nm, five scans were averaged over 3 s integration time. All the spectra were buffer subtracted and intensity-normalized at the peak maximum to visualize the spectral-shifts using OriginPro Version 8.5 software.

2.7.2 Tryptophan quenching experiments:

For tryptophan quenching experiment, KI (potassium iodide) was used as a quencher. 5 M stock solution of KI containing 250 μM of sodium thiosulphate ($Na_2S_2O_3$) was prepared in MilliQ water and was diluted to a final concentration of 200 mM. The variant A78W was chosen for quenching experiment, since it showed high REES. The concentration of A78W α-synuclein mutant and SUVs were 50 μM and 2 mM, respectively. The tryptophan emission was observed in the presence and in the absence of KI. Following parameters were fixed for collecting tryptophan scans: λ_{ex} = 295 nm and λ_{em} scan range was from 310 nm to 400 nm. The excitation and emission bandpass were

adjusted to 0.5 nm and 3 nm, respectively. The integration time was fixed at 1 s and averaged over three scans. All the spectra were buffer subtracted and intensity-normalized at the peak maximum to visualize spectral-shifts using OriginPro Version 8.5 software.

2.7.3 Membrane dipole potential measurements:

For membrane dipole potential experiments, the concentration of SUVs were kept constant at 2 mM in DPBS buffer, whereas, variable concentrations of α-synuclein (viz. 10 μM, 50 μM and 100 μM) were used. di-8-ANEPPS was used as a voltage sensitive styrylpyridinium probe and the dipole potential measurements were performed by dual wavelength ratiometric approach.[20,21] 500 μM stock solution of di-8-ANEPPS was prepared in ethanol and diluted to a final concentration of 5 μM. Two excitation wavelengths of 420 nm and 520 nm were used and emission was fixed at 670 nm with an integration time of 2 s. The excitation bandpass and emission bandpass were fixed to 1 nm and 2 nm, respectively. All samples (with protein and POPG) were incubated with di-8-ANEPPS for 1 hour before collecting the data. Dipole potential in mV was calculated from R (Ratio of emission at 670 nm, exciting at 420 nm and 520 nm) using the following relationship:[21]

$$\Psi_d = (R + 0.3) / (4.3 \times 10^{-3}) \quad (2)$$

2.8 Time-resolved fluorescence measurements:

The time-resolved fluorescence decays of the samples (in the absence and presence of Trp variants in POPG) were collected using a time correlated single-photon-counting (TCSPC) setup (Fluorocube, Horiba Jobin Yvon, NJ). 295 nm LED (Light Emitting Diode) was used as excitation source having repetition rate of 1 MHz. All the decays were collected at magic angle (54.7°) with 12 nm bandpass and a PhotoMultiplier Tube (PMT) (Hamamatsu Corp) was used as detector. An aqueous solution of 2 % ludox was used to collect the instrument response function (~1.1 ns). In order to obtain a good signal-to-noise ratio, 10,000 counts were collected at the peak. All the experiments were carried out at room temperature.

2.8.1 Tryptophan fluorescence intensity decay:

For all the life time measurements, the concentration of α-synuclein mutants and SUVs of POPG were kept constant in DPBS buffer, as 50 μM and 2 mM respectively. Cuvette (from Helma) of pathlength 10 mm x 2 mm was used. Tryptophan decay was collected in the presence and in the absence of α-synuclein variants at 335 nm. The intensity decay were collected and analyzed.

2.8.2 FRET (Fluorescence resonance energy transfer):

For fluorescence resonance energy transfer (Trp → NBD) measurements, the concentration of α-synuclein mutants and 5 % NBD-PE labeled-POPG SUVs were kept constant in DPBS buffer, as 50 μM and 2 mM, respectively. A cuvette (from Helma) of pathlength 10 mm x 2 mm was used for the measurements. The tryptophan decay was collected at 335 nm for all the variants. The tryptophan decay in the presence and in the absence of labeled SUVs were collected and analyzed. The FET efficiencies (E) were estimated from the lifetime of Trp in the absence of acceptor (τ_D) and in the presence of acceptor (τ_{DA}) using the following relationship.

$$E = 1- (\tau_{DA}/\tau_D) \quad (3)$$

2.8.3 TRES (Time Resolved Emission spectra) – measurement and analysis:

The TRES measurement was carried out for A78W α-synuclein mutant (50 μM) with POPG SUVs (2 mM) in DPBS buffer in a cuvette of pathlength 10 mm x 10 mm. The tryptophan intensity decays were collected in the wavelength range from 315 nm to 360 nm with an interval of 5 nm. The tryptophan intensity decays were deconvoluted with respect to IRF (Instrument Response Function) and analyzed by fitting them as a sum of exponentials. The fits were used to construct the TRES. The spectra were normalized and fitted to logarithm normal function using OriginPro V8.5 software.

2.9 Tryptophan fluorescence anisotropy decay:

Time-resolved anisotropy decay measurements of the samples were made using a picosecond laser Ti: sapphire laser (Tsunami, Spectra Physics) coupled to a time-correlated single-photon-counting setup.[40] A frequency tripled output of 885 nm was used to excite Trp at 295 nm. The IRF at 295 nm was collected using a dilute colloidal suspension of dried nondairy whitener. The width of the IRF was ~ 40 ps. For the anisotropy decay measurements, the emission data were collected at 0° and 90° with respect to the excitation polarization. NATA solution was to estimate the G-factor. The emission monochromator was fixed at 335 nm for F4W and A56W, whereas, for A140 W it was fixed at 350 nm with a bandpass of 20 nm. A 320 long-pass filter was placed just after the sample to block any scattering from the sample. The anisotropy decays were analyzed by globally fitting $I_{\parallel}(t)$ and $I_{\perp}(t)$ as follows:

$$I_{\parallel}= \frac{I(t)[1+2r(t)]}{3} \quad (4)$$

$$I_{\perp}= \frac{I(t)[1-r(t)]}{3} \quad (5)$$

The perpendicular component of the fluorescence decay was corrected for the G-factor of the spectrometer. I(t) is the fluorescence intensity collected at the magic angle (54.7) at time t. The anisotropy decays were analyzed using a biexponential decay model describing fast and

slow rotational correlation times as follows:

$$r(t)=r_o[\beta_{fast}\exp(-t/\phi_{fast}) +\beta_{slow}\exp(-t/\phi_{slow})] \quad (6)$$

where r_o is the intrinsic fluorescence anisotropy; ϕfast and ϕslow are the fast and slow rotational correlation times; and β_{fast} and β_{slow} are the amplitudes associated with fast and slow rotational time. The global (slow) rotational correlation time (ϕ_{slow}) is related to viscosity (η) and molecular volume (V) by the Stokes-Einstein relationship as follow:

$$\phi_{slow}=\eta V/kT \quad (7)$$

$$V=4/3\Pi R_h^3 \quad (8)$$

where R_h is the hydrodynamic radius of the molecule.

3. Results and discussion:

3.1 Binding-induced folding of α-synuclein at the lipid membrane surface:

The study was initiated by performing Circular dichroism (CD) of α-synuclein in the absence and in the presence of lipid membrane (Figure 2). We have chosen POPG SUVs, since it is known to bind to α-synuclein with highest affinity[22,23]. We observed a transition from random coil state to a highly helical state upon binding with SUVs derived from POPG. This preliminary result prompted us to understand this conformational change in residue specific manner.

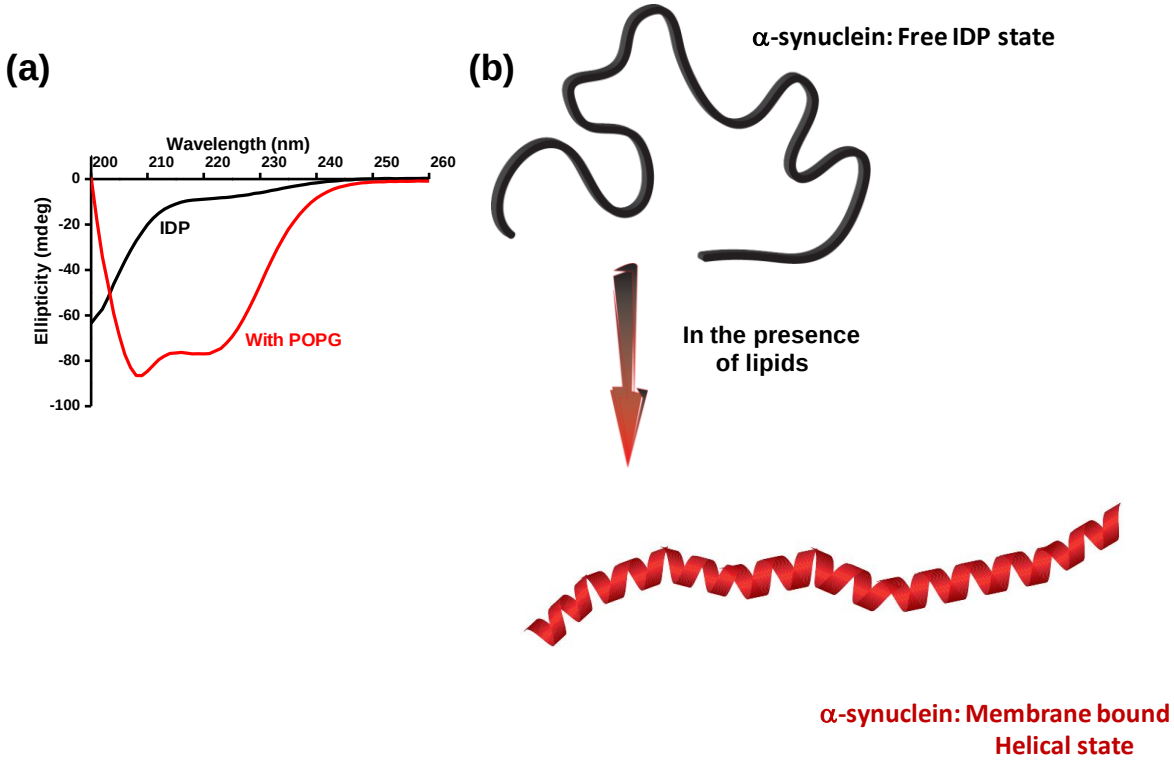

Figure 2. CD spectra of wild-type α-synuclein. (a) Change in secondary structure from random coil (Black: Native) to α-helix with POPG (Red) (b) Schematic diagram to show the transition from IDP to helical state.

Since α-synuclein is binding to the outer surface of the POPG SUVs, so we asked, if is there any effect on the ordering of the lipid head-groups. To address this question, we measured the dipole potential of lipid membranes derived from POPG in the absence and in the presence of α-synuclein. The change in the dipole potential arises because of non-random arrangements of ester groups linked to the glycerol backbone of phospholipids

and usually ranges between 200-500 mV depending on the lipids.[24]Using a ratiometric fluorescent reporter, di-8-ANEPPS (a charge transfer dye).[25]

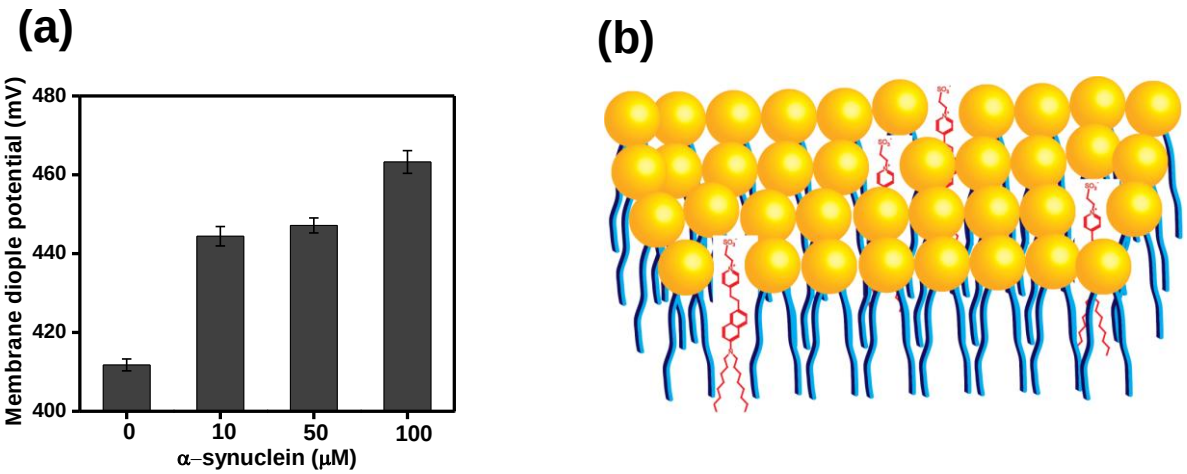

Figure 3. (a) Measurement of membrane dipole potential using di-8-ANEPPS at different concentrations of α-synuclein. (b) Schematic representation of the membrane bilayer showing the localization of di-8-ANEPPS in the membrane.

We measured the dipole potential of POPG membrane. The schematic representation of binding of di-8-ANEPPS with the membrane is given in Figure 3(b). We observed an increase of 30-50 mV dipole potential in the presence of α-synuclein depending upon the protein concentration (Figure 3(a)). These results demonstrated that α-synuclein upon binding to POPG SUVs, undergoes some conformational rearrangement that lends ordering of phospholipids.

3.2 Structural and dynamical insights into the membrane-bound state of α-synuclein:

The above interesting results from CD and membrane potential lead us to perform further experiments to understand the residue specific structural dynamics of α-synuclein in membrane-bound state.

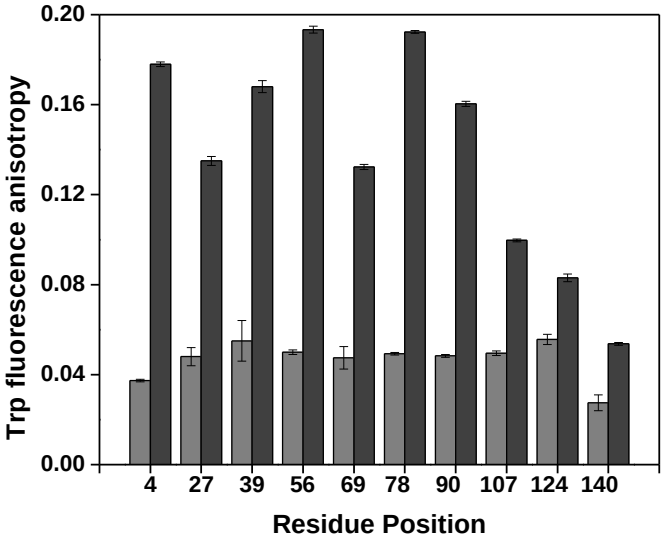

Figure 4. Tryptophan fluorescence anisotropy in the absence (light gray) and in the presence of POPG SUVs (dark gray).

We took the advantage of the fact that α-synuclein is devoid of any tryptophan (Trp) residue. So, 10 single-Trp mutants were generated over the polypeptide chain length. For incorporating Trp, the residue positions at 4, 39, 69, 90, 124 and 140 were chosen based on earlier reports[26] due to conservative exchange of amino acid. We made additional four single Trp mutants (27, 56, 78 and 107) which maintain disordered structure of protein in unbound form and form helical structure in bound form to POPG SUVs. Previous studies from the lab have demonstrated that these mutants behave like the wild-type protein. [22] In the free form, anisotropy was low (0.05 ± 0.01) for all the Trp variants, which indicates that the protein exist in the disordered form (Figure 4). Based on this experiment, we revealed that the N-terminal end is tightly bound and structured, whereas, C-terminal end does not seem to participate in the folding event. The middle region of the N-terminal segment (Trp 27 and 39) showed a higher degree of flexibility, while the region juxtaposing the N- and the NAC-domain (Trp 78) is highly structured as indicated by high anisotropy. The NAC-domain also showed different degrees of structural organization. The initial region (Trp 69) showed a lower degree of structure as compared to the middle region (Trp 78). The anisotropy of the mutants after Trp 78 progressively decreases as Trp is moved from the NAC- to the C-terminal region. This experiment provides residue-specific structural organization of the α-synuclein upon the POPG SUVs.

We have carried out picosecond time-resolved fluorescence anisotropy measurements that provide insights into the local and global rotational dynamics of proteins.[27,28]Global dynamics is represented by a slow rotational correlation time (ϕ_{slow}) that is generally related to the size (hydrodynamic radius) of the protein (Eq. 6-8). In the unbound form, α-synuclein showed two rotational correlation times. The fast rotational correlation time, ϕ_{fast} is ~ 0.13 ns and 0.14 ns for F4W and A124W, respctively, (Table 1) which represents the local dynamics of Trp, whereas ϕ_{slow} is 1.1 ns and 1.56 ns for F4W and A124W, respectively, and could indicate the segmental mobility and does not depend on the protein size, since the segmental conformation fluctuations depolarize the fluorescence much more rapidly than the global tumbling of the polypeptide chain.[28] For the membrane bound variants of the protein, ϕ_{slow} increased to ~ 45 ns for F4W variants, whereas, for A124W variant it is around 1.3 ns. These results indicates that the α-synuclein is tightly bound to the position near 4 amino acid, whereas, the 124th residue (C-terminal variant of α-synuclein) is not bound to the membrane.

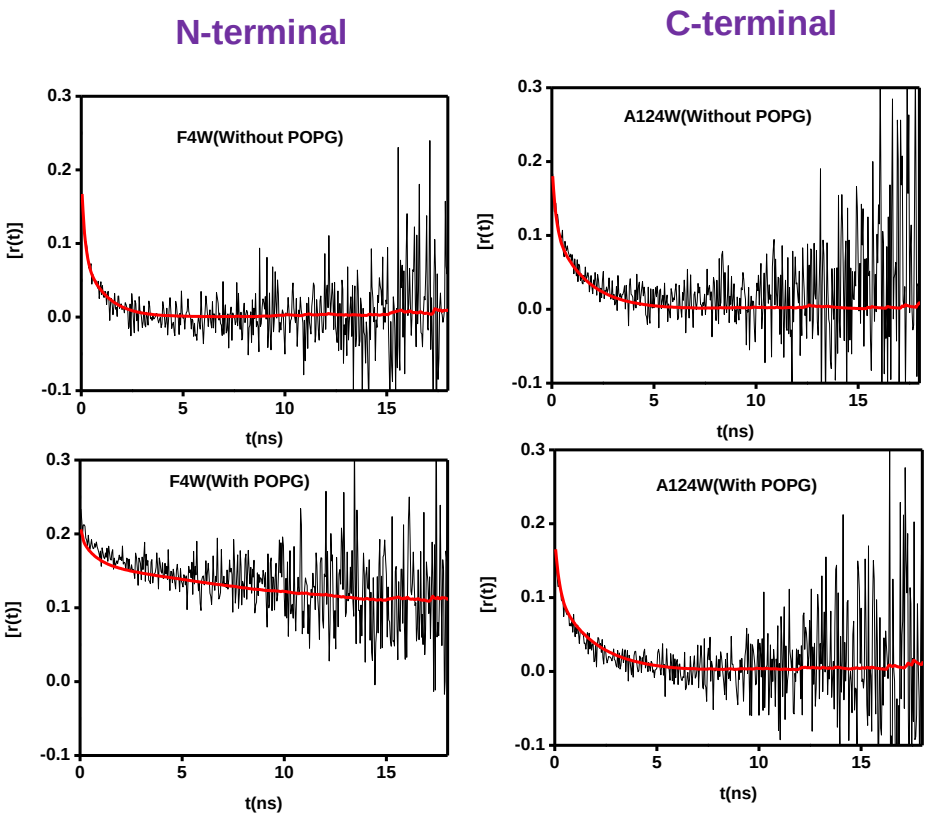

Figure 5. (a) Picosecond time-resolved fluorescence anisotropy decays [r(t)] in the presence and absence of POPG LUVs of F4W (lane 1) and A124W (lane 2). The solid red line is the biexponential fit (Eq. 6).

Table 1. Tryptophan fluorescence life time and rotational correlation times for two single-Trp mutants of α-synuclein (F4W and A124W) in the absence and in the presence of lipid membranes.

Trp Variants (Conditions)	**Fluorescence Lifetime in ns (amplitude)**			**Mean Lifetime in ns**		**Rotational Correlation time in ns (amplitude)**				
	τ_1 (α_1)	τ_2 (α_2)	τ_3 (α_3)	τ_{av}	χ^2	φ_1 (β_1)	φ_2 (β_2)	r_0	r_{ss}	χ^2
F4W (free; native)	4.13 (0.37)	1.9 (0.43)	0.51 (0.20)	2.4	1.13	1.1 (0.44)	0.13 (0.56)	0.2	0.03	1.9
F4W (with SUVs)	3.9 (0.50)	1.61 (0.36)	0.39 (0.14)	2.6	1.12	44.8 (0.76)	0.56 (0.24)	0.208	0.156	1.9
A124W (free; native)	3.51 (0.34)	1.87 (0.44)	0.65 (0.22)	2.16	0.99	1.56 (0.53)	0.14 (0.47)	0.211	0.05	1.9
A124W (with SUVs)	4.14 (0.20)	2.2 (0.56)	0.65 (0.24)	2.22	1.2	1.32 (0.52)	0.15 (0.48)	0.213	0.044	1.9

The anisotropy decay for the F4W in the membrane-bound form did not completely depolarize in the timescale of Trp fluorescence. The tumbling of the SUV-protein complex is much slower (on the μs timescale). Whereas, in the case of A124W variant in membrane bound form, anisotropy of Trp decayed to zero indicating fast tumbling (Figure 5) and this location is far away from the membrane-binding site.

3.3 The depth profile of α-synuclein on the membrane surface:

The above results prompted us to perform experiments that would allow us to distinguish the proximal and distal tryptophan with respect to the membrane surface. One of the fluorescence readouts is the red-edge excitation shift (REES), it is generally observed with polar fluorophores in motionally restricted media (or with liposome) where the dipole relaxation time for the solvent shell around a fluorophore is comparable to or longer than its fluorescence lifetime (nanoseconds). The emission maxima exhibit a progressive shift towards the longer wavelength, when excitation wavelength shifted to the red edge of the absorption band. In the disordered state, Trp residues placed along the sequence showed very little or no REES, whereas, in the membrane-bound form, different residue positions demonstrated a varied extent of REES. This was previously demonstrated in our lab.[22] The REES experiments were repeated before carrying out time-resolved emission spectra (TRES) measurements that provide direct evidence of slow water relaxation. For REES measurements, the fluorescence spectra were collected by exciting Trp of POPG-bound α-synuclein (Trp 78 and 140) at three different wavelengths (280 nm, 295 nm and 305 nm) at the red-edge of the tryptophan absorption maxima (Figure 6a). In the spectra, progressive shift in the emission maxima for Trp 78 variant was observed as a function of excitation wavelength. Trp 140 which is located at the end of C-terminus did not undergo detectable shift. We plotted the REES (in nm) for each residue position in the membrane-bound form to construct a *dynamic hydration map* (Figure 6b). Initial part of the N-terminal sequence (Trp 4) demonstrated a large extent of the REES (~13 nm), whereas, the middle region (Trp 27 and 39) exhibited much lower REES. In the NAC-domain, residues 78 and 90 showed a significant REES (~ 15 nm and 11 nm, respectively), whereas, the residue 69 exhibited much lower REES (~ 5 nm).

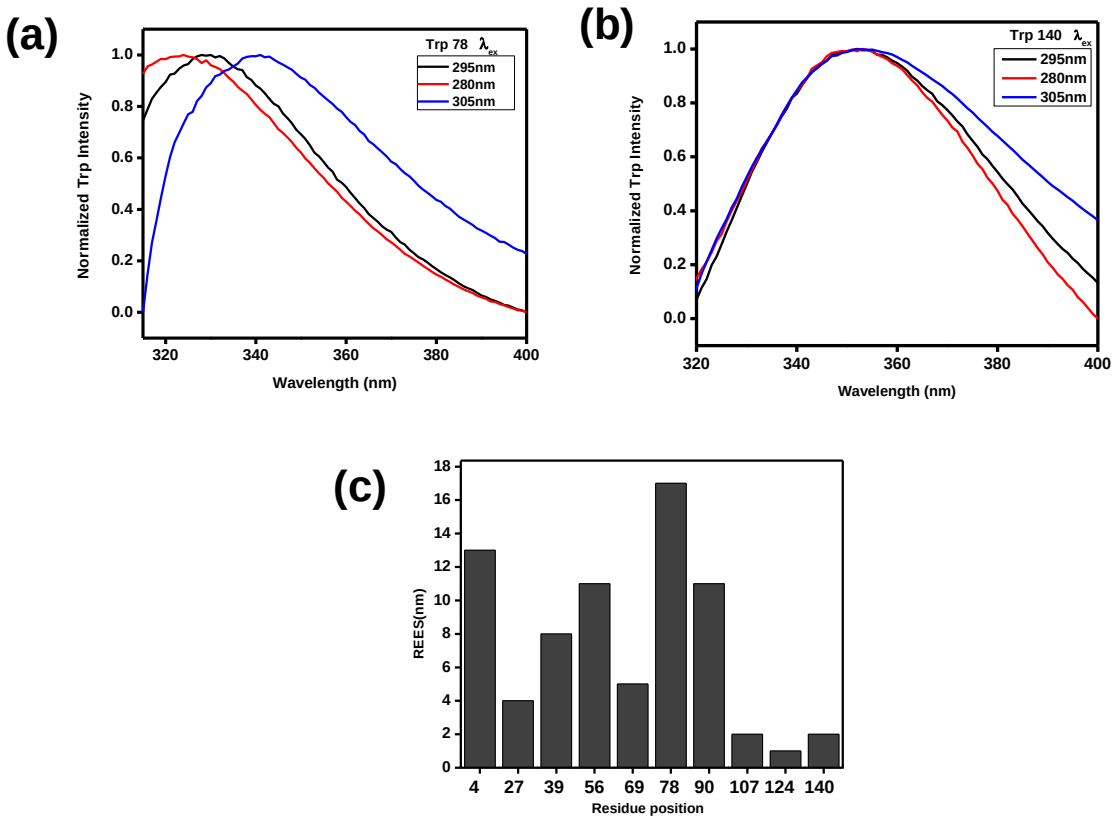

Figure 6. (a), (b) Spectral shift with progressive change in excitation wavelength (l_{ex}=280, 295, 305) for two mutants (A78W and A140W) in the presence of POPG SUVs. (c) Extent of REES observed with all Trp variants in the presence and in the absence of POPG.

The C-terminal residues did not show any significant REES. We would like to point out that the shift can also arise due to a structural heterogeneity.

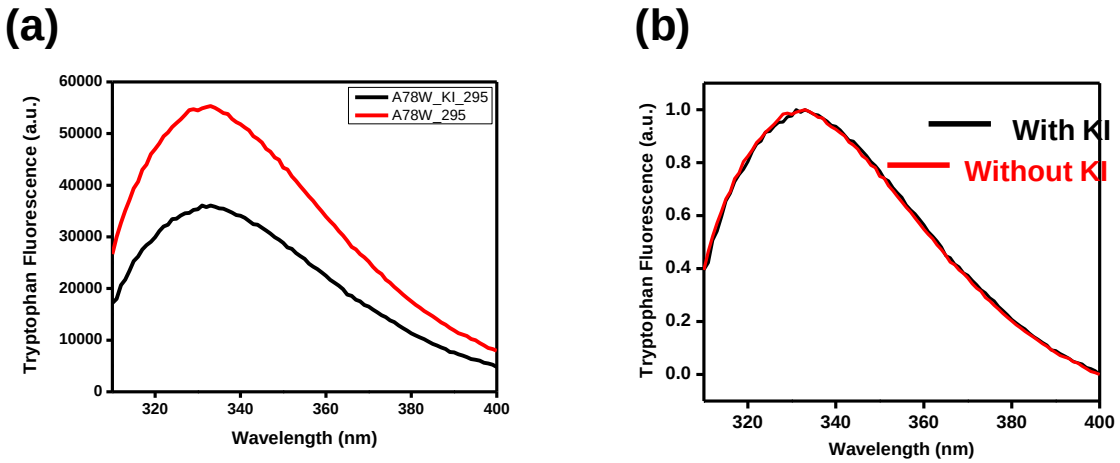

Figure 7. (a) Tryptophan fluorescence spectra of A78W mutant in the absence and in the presence of quencher (KI). (b) Intensity normalized Tryptophan fluorescence spectra of A78W mutant in the presence and absence of KI to visualize the spectral shift.

In order to rule out this possibility, we carried out a control experiment with Trp 78 mutant that exhibited maximum extent of REES. We recorded fluorescence spectra in the absence and in the presence of a quencher (potassium iodide) and observed that the spectral shape and emission maximum remains unaltered (Figure 7). Therefore, the REES observed was indeed due to slow water reorientation dynamics and not due to any structural heterogeneity. The schematic model for the unbound (Native) and membrane bound form of the α-synuclein is shown in Figure 10.

3.4 TRES measurements to provide direct insights into the water dynamics at the membrane-water interface felt by membrane-bound α-synuclein:

As mentioned before, REES arises due to the rate of water reorientation dynamics that is either comparable to or slower than the fluorescence lifetime. In order to directly monitor the water dynamics, we next embarked upon studying the timescale of hydration dynamics of α-synuclein in the presence of POPG SUVs using time-resolved emission spectra (TRES) that measures the time-dependent Stokes shift (TDSS) on the nanosecond timescale. In order to perform TRES experiments, we decided to use Trp 78 variant due to its maximum extent of REES. The time-resolved decay of Trp fluorescence was monitored at different emission wavelength. It was observed that the fluorescence decay become progressively longer with an increase in the average fluorescence lifetime as a function of emission wavelength (Figure 8).

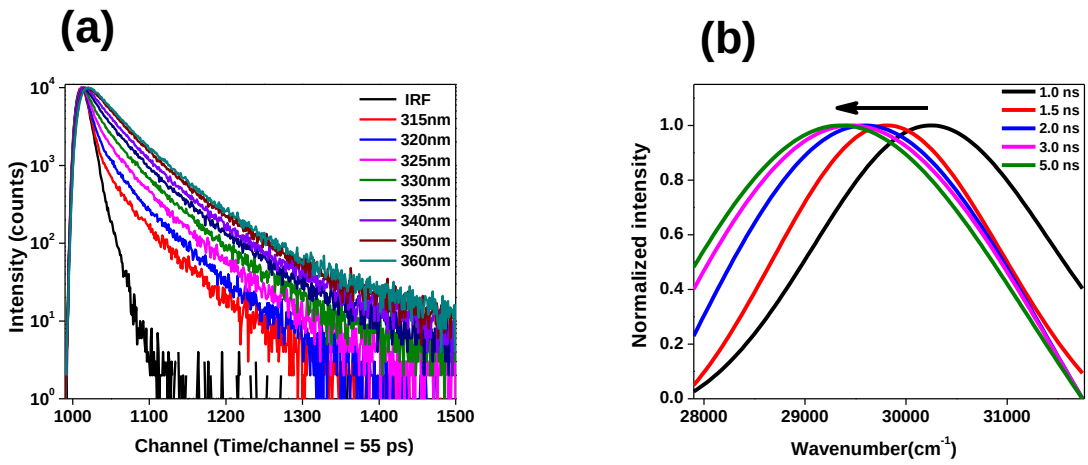

Figure 8. Trp 78 in presence of POPG: (a) The time resolved decay of Trp fluorescence monitored at different wavelengths (b) Time resolved emission shift (TRES) constructed from life time decays.

The TRES constructed from the decay analysis exhibited TDSS on the nanosecond timescale. These results provided compelling evidence in favour of ultraslow water relaxation arising from localization of the Trp-residue at membrane-interface comprising a highly ordered water layer with a constrained mobility.

3.5 Proximity between various residues of α-synuclein and membrane surface monitored by FRET:

To gain more information about the positioning of residues on the membrane surface, we performed FRET (between NBD labeled membrane and Trp variants of the α-synuclein) experiments. NBD and Trp acts as a FRET pair with a Förster's distance value, determined is 22 Å as reported.[29]The schematic model for the FRET is shown in Figure 9(b) N- and NAC regions showed variable but high FRET efficiency, whereas, C region showed less FRET efficiency (Figure 9(a)).

Initial part of the N-terminal sequence (Trp 4) demonstrated a large FRET efficiency (~50%), Whereas, the middle region (Trp 27) exhibited little less FRET (~30%). In the NAC-domain, residues 78 and 90 showed a significant FRET efficiency (53% and 40%, respectively), whereas, the residue 69 exhibited much lower FRET (~23%). The C-terminal residues showed some FRET efficiency. Our FRET results by enlarge corroborated with the anisotropy and REES experiments

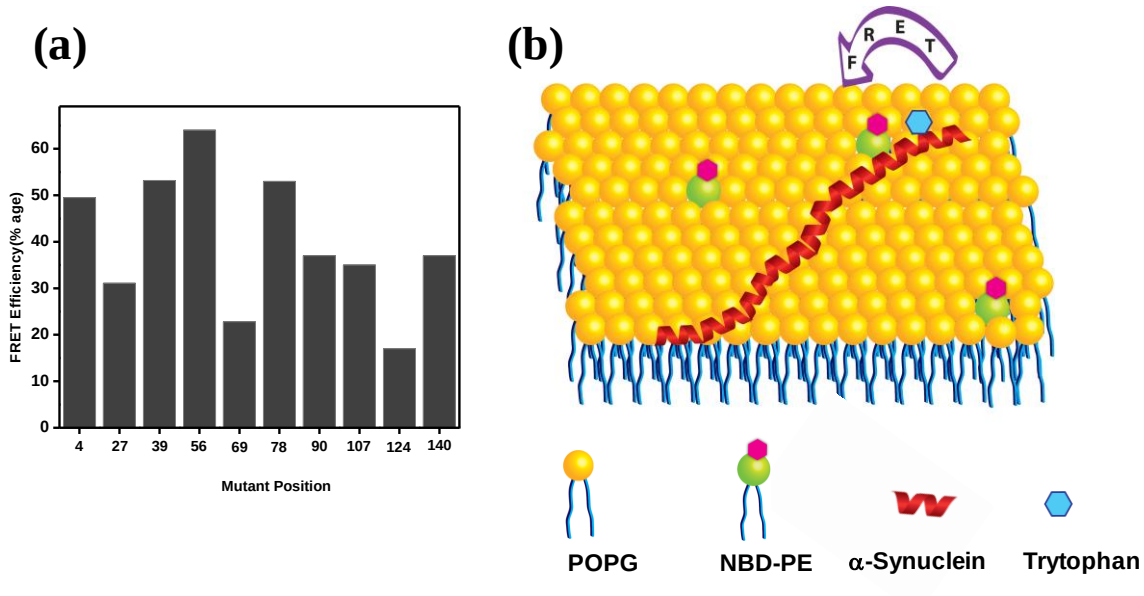

Figure 9. (a) FRET efficiency observed with different tryptophan mutants. (b) A schematic representation of FRET between protein and membrane.

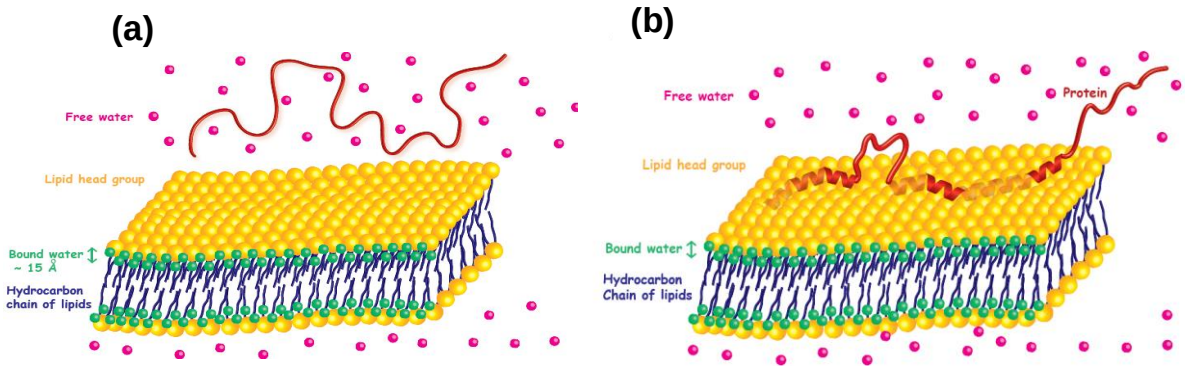

Figure 10. Schematic representation (a) Unbound α-synuclein (b) α-synuclein bound to membrane

3.6 Co-assembly of Tau and α-synuclein Protein:

Tau and α-synuclein are present in different locations in the neuron. It has been reported that α-synuclein is capable of membrane translocation[30,31] and fibrillated form may be transferred between neurons.[32,33]We initiated the study by monitoring aggregation of Tau

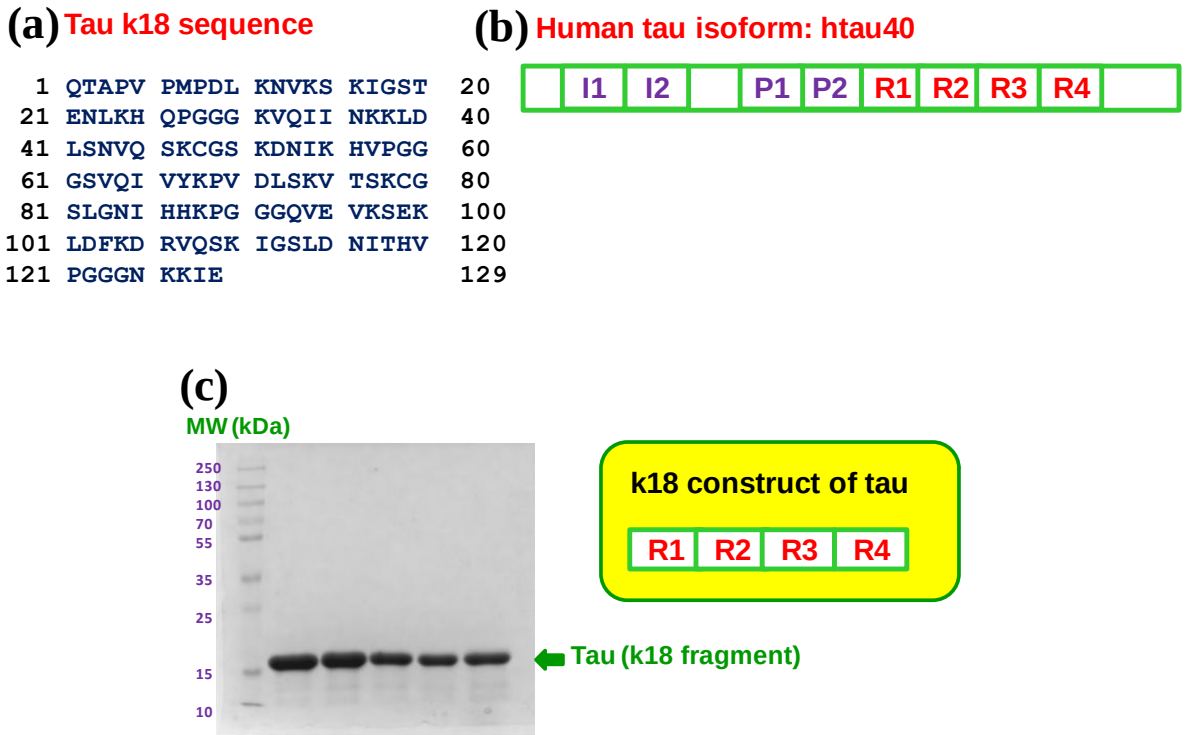

Figure 11. (a) Sequence of Tau (k18) (b) A schematic map of full length Tau [I: Insert region, P: Proline rich region & R: Repeat region] (c) Tau (k18) protein pure fractions.

and α-synuclein separately under identical conditions. We observed no significant increase in Tht intensity which is an indicator of fibril formation (Figure 12a).

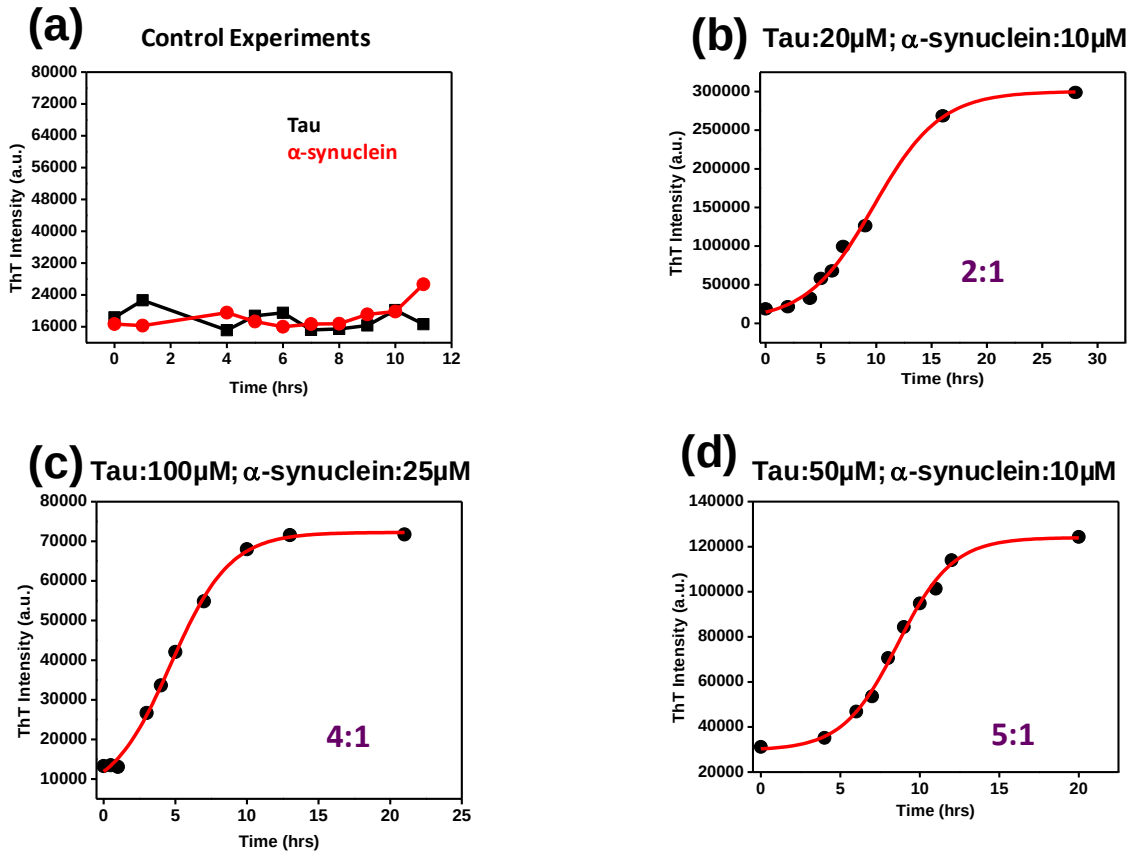

Figure 12. (a) Control experiment (with only Tau and only α-synuclein). (b) Tau:α-synuclein ratio 2:1 (c) Tau:α-synuclein ratio 4:1 and (b) Tau : α-synuclein ratio 5:1

Next we took both the proteins in the same reaction at different protein ratios and found that the Tht intensity was greatly enhanced and reached to plateau after ~ 20 hours (Figure 12 b,c,d).The proposed reason for the coaggregation could be due the electrostatic interaction, because Tau is positively charged at physiological pH, whereas, α-synuclein is negatively charged. This observation suggested that some conformational changes in the proteins (tau and α-synuclein) drive the aggregation process. Though, at present it is difficult to answer which one of the two proteins initiates the process. To address this question we plan to generate cysteine mutations in α-synuclein which when labeled with TNB can act as FRET pair for Trp mutations generate in Tau protein. Utilizing this system we aim to answer some of the questions pertaining co-aggregation of Tau and α-synuclein.

4. Conclusion and Future Outlooks:

The prevailing concept in IDPs is that the conformational plasticity allows proteins to adopt different structure when they come in contact with different binding partners. α-synuclein adopts a helical structure when it binds to lipid membranes. However the high-resolution structural and dynamical insight of the membrane bound structure was not fully understood. In the present study, fluorescence anisotropy, REES, TRES and FRET results have revealed the intricate structural details of α-synuclein on the negatively charged membrane. Our results elucidate the precise conformation of the α-synuclein protein on the negatively charged membrane which might have implications in some of its putative physiological functions. For instance, it has been proposed that the membrane-bound α-synuclein helps in synaptic transmission and the C-terminal segment interact with a SNARE (soluble N-ethyl maleimide sensitive factor attachment protein receptors) complex protein known as synaptobrevin which helps in neurotransmitter release. Region-specific binding and folding of α-synuclein to the membrane surface can influence the membrane stability and fluidity.[34] It has been known that A30P, missence mutation in α-synuclein gene results in Parkinson's disease.[35,36,37] The region near 27 and 39 and residue 30 come in-between may be this structurally broken segment of the protein facilitates protein aggregation on the membrane surface. Additionally, tau and α-synuclein accumulate to form fibrils that are pathological inclusions in distinct neurodegenerative disorders now classified as tauopathies and synucleinopathies, respectively.[38,39] Our results showed the different aggregation propensity at different ratios of both the proteins. So, this work can further be extended to understand the precise mechanism of co-assembly that has a myriad of important implications in neurodegenerative diseases.

5. Bibliography:

1. Demchenko AP (2008) Site-selective red-edge effects. Methods Enzymol. 450:59-78.

2. Haldar S, Chaudhuri A, Chattopadhyay A (2011) Organization and dynamics of membrane probes and proteins utilizing the red edge excitation shift. J. Phys. Chem. B 115:5693-5706.

3. Uversky VN (2002) Natively unfolded proteins: a point where biology waits for physics. Protein Sci. 11:739–756.

4. Iakoucheva LM, Brown CJ, Lawson JD, Obradović Z, Dunker AK (2002). "Intrinsic disorder in cell-signaling and cancer-associated proteins". J. Mol. Biol. 323 (3):573–84.

5. Weinreb PH, Zhen W, Poon AW, Conway KA, Lansbury PT, Jr, (1996) NACP, a protein implicated in Alzheimer's disease and learning, is natively unfolded. Biochemistry 35:13709-13715.

6. Tamamizu-Kato S, et al. (2006) Calcium-triggered membrane interaction of the α-synuclein acidic tail. Biochemistry 45:10947-10956.

7. Abeliovich A (2000) Mice lacking α-synuclein display functional deficits in the nigrostriatal dopamine system. Neuron 25:239-252.

8. Cooper AA et al. (2006) α- Synuclein blocks ER-Golgi traffic and Rab1 rescues neuron loss in Parkinson's models. Science 313:324-328.

9. Watson JB (2009) Alterations in corticostriatal synaptic plasticity in mice over-expressing human α-synuclein neuroscience. Neurosci. 159:501-513.

10. Eliezer D, Kutluay E, Bussell R, Jr, Browne G (2001) Conformational properties of α-synuclein in its free and lipid-associated states. J. Mol. Biol. 307:1061-1073.

11. Chandra S, Chen X, Rizo J, Jahn R, Sudhof TC (2003) A broken α-helix in folded α-synuclein. J. Biol.Chem. 278:15313-15318.

12. Bortolus M et al. (2011) Direct evidence of coexisting horseshoe and extended helix conformations of membrane-bound alpha-synuclein. ChemPhysChem 12:267-269.

13. Goedert M, Spillantini MG, Jakes R, Rutherford D, Crowther RA (1989). Multiple isoforms of human microtubule-associated protein tau: sequences and localization in neurofibrillary tangles of Alzheimer's disease". Neuron 3 (4):519–26.

14. Alonso A, Zaidi T, Novak M, Grundke-Iqbal I, Iqbal K (2001). Hyperphosphorylation induces self-assembly of tau into tangles of paired helical filaments/straight filaments. Proc. Natl. Acad. Sci. U.S.A. 98 (12):6923–8.

15. Averbeck BB, Lee D (2004) Coding and transmission of information by neural ensembles. Trends Neurosci. 27(4):225-30.

16. Giasson BI, Lee VM, Trojanowski JQ (2003). Interactions of amyloidogenic proteins. Neuromolecular Med. 4 (1-2):49–58.

17. Van Raaij ME, Ine MJ, Segers-Nolten, I. M. J.; Subramaniam, V. (2006) Quantitative morphological analysis reveals ultrastructural diversity of amyloid fibrils from α-synuclein mutants. Biophys. J. L96-98.

18. Pfefferkorn CM et al. (2012) Depth of α-synuclein in a bilayer determined by fluorescence, neutron reflectometry, and computation. Biophys. J. 102:613-621.

19. Drescher M et al. (2008) Antiparallel arrangement of the helices of vesicle-bound a-synuclein, J. Am. Chem. Soc. 130:7796-7797.

20. Starke-Peterkovic T, Turner N, Else PL, Clarke RJ (2005) Electric field strength of membrane lipids from vertebrate species: membrane lipid composition and Na+-K+-ATPase molecular activity. Am J Physiol Regul Integr Comp Physiol. 288(5):R1422

21. Gross E, Bedlack, Jr RS, Loew LM (1994) Dual-wavelength ratiometric fluorescence measurement of the membrane dipole potential. Biophys J. 67(1): 208–216.

22. Ph.D. Thesis (2013) Neha Jain.

23. Wang GF, Li C, Pielak GJ (2010) 19F NMR studies of α-synuclein-membrane interactions. Prot. Sci.19:1686-1691.

24. Demchenko AP (2008) Site-selective red-edge effects. *Methods Enzymol.* 450:59-78.

25. Gross E, Bedlack Jr RS, Loew LM. (1994) Dual-wavelength ratiometric fluorescence measurement of the membrane dipole potential. Biophys. J. 67:208-216.

26. Pfefferkorn CM, Lee JC. (2010) Tryptophan probes at the a-synuclein and membrane interface. J. Phys. Chem. B. 114:4615–4622.

27. Lakowicz, J. R. 2006. Principles of Fluorescence Spectroscopy, 3rd ed. Springer, New York.

28. Saxena A, Udgaonkar JB, Krishnamoorthy G. (2005). Protein dynamics and protein folding dynamics revealed by time-resolved fluorescence. In Fluorescence Spectroscopy in Biology. Advanced) Methods and their Applications to Membranes, Proteins, DNA,

and Cells. M. Hof, R. Hutterer, and V. Fidler, editors. Springer-Verlag, New York. 163–179.

29. Cabré EJ , Loura LMS, Fedorov A,Perez-Gil J, Prieto M (2012) Topology and lipid selectivity of pulmonary surfactant protein SP-B in membranes: Answers from fluorescence Biochimica et Biophysica Acta. 1818(7):1717-1725.

30. Ahn KJ, Paik SR, Chung KC, Kim J (2006) Amino acid sequence motifs and mechanistic features of the membrane translocation of α-synuclein. Journal of Neurochemistry. 97: 265-297

31. Liu G et al. (2009) Alpha-Synuclein is differentially expressed in mitochondria from different rat brain regions and dose-dependently down-regulates complex I activity. Neurosci. Lett. 454 (3): 187–92.

32. Desplats P et al. (2009) Inclusion formation and neuronal cell death through neuron-to-neuron transmission of α-synuclein. PNAS 106:13010 –13015

33. Boland B. et al.(2008) Autophagy Induction and Autophagosome Clearance in Neurons: Relationship to Autophagic Pathology in Alzheimer's Disease. JNEUROSC.I 28(27): 6926-6937

34. Ulmer TS, Bax A, Cole NB, Nussbaum RL (2005) Structure and dynamics of micellebound human α-synuclein. J.Biol.Chem. 280:9595-9603.

35. M. H. Polymeropoulos et al. (1997) Mutation in the α-Synuclein Gene Identified in Families with Parkinson's Disease. Science 276:2045-2047.

36. Kruger R et al.(1998) Ala30Pro mutation in the gene encoding alpha-synuclein in Parkinson's disease. Nat. Genet. 18(2):106-1088.

37. Zarranz JJ et al.(2004) The new mutation, E46K, of alpha-synuclein causes Parkinson and Lewy body dementia. Ann. Neurol. 55(2):164-73.

38. Lee VMY, Goedert M, Trojanowksi JQ (2001) Neurodegenrative Taupathies Annu.Rev. Neurosci. 24:1121-1159

39. Bue´e L, Bussie`re T, Bue´e-Scherrer V, Delacourte A, Hof PR (2000) Formation of neurofibrillar tangles P301L tau transgenic mice induces by Aβ42 fibrils. Brain Res. Rev. 293: 1491-1495

40. Mukhopadhyay S,Nayak P, Udgaonkar JB, Krishnamoorthy G.(2006) Characterization of amyloid fibril formation by mapping residue-specific fluorescence dynamics. J. Mol. Biol. 358: 935-942.